Bull. Disas. Prev. Res. Inst. Kyoto Univ., Vol. 16, Part 3, No. 115, March., 1967

On the Characteristics of Flood Waves under various Boundary Conditions

By Kazuo ASHIDA and Tamotsu TAKAHASHI

(Manuscript received December 10, 1966)

Abstract

The behavior of the flood flow in a river is very complex because of the effects of various kinds of boundary or channel conditions. To clarify these effects on the flood a series of experiments were conducted in a flume (150 m in length, 60 cm in width and in depth) at the downstream end of which a few kinds of boundary condition were set. By means of these experiments and appropriate theoretical considerations authors have been able to discuss the characteristics of flood flow under the following boundary conditions:

a) at $x\to\infty$, $h\to 0$ b) at $x=l$, $h=0$ c) at $x=l$, $h=h(q)$ d) at $x=l$, $h=h(t)$

where x is distance, t time, h the water depth measured above the stage of steady base flow, q the discharge per unit width, and $h(q)$, $h(t)$ are the given single valued functions of q and t respectively.

1. Introduction

Various kinds of analysis for flood flow have been conducted since the last century, and the behavior of flood flow that propagates itself through a prismatic channel can be almost completly predicted by theoretical methods. These methods are applicable to the flood in a natural river, when its irregularity is not very strong and it can be considered to be prismatic on the average. But there are many places which we can not consider to be prismatic, even on average, as when there is a sudden change of channel form or slope, channel junction, estuary, reservoir, etc. In these regions the terms of the equation of motion which are negligible in a prismatic channel become important and the analytical methods adopted for a prismatic channel are no longer valid. Therefor, to clarify the properties of flood flow in these regions is one of the most important problems of hydraulics and river engineering. But it is very difficult, and up to the present, the phenomena in a specific case have mainly been understood through solving the equation of motion and continuity under given initial and boundary conditions with the help of a digital or analog computor. Through the accumulation of these studies the general properties of flood flow will gradually be made clear, but generally in the fundamantal equation that is adopted some kinds of abbreviations are included and we must always discuss the validity of this equation, and so before using those computors we must understand the characteristics of the fundamental equation and the phenomena themselves.

On the other hand some experimental and theoretical studies for these cases have been carried out and have achieved good results, for example the analysis

for the case of the combination of flood flow and tide or storm surge and the studies of the deformation of flood flow propagated through a reservoir, but the quantitative estimation of the effect of a boundary condition is still impossible.

Considering the above-mentioned state of knowledge, the authors started a series of experimental and theoretical studies to discover the properties of flood flow under various kinds of conditions.

This paper deals with flood flow, under the following boundary conditions:

a) at $x\to\infty$, $h\to 0$
b) at $x=l$, $h=0$
c) at $x=l$, $h=h(q)$
d) at $x=l$, $h=h(t)$,

where x and l are distances, t time, h the water depth measured above the stage of steady base flow, q the discharge per unit width, and $h(q)$, $h(t)$ are the given single valued functions of q and t respectively.

The flood through a prismatic channel which is usually treated under condition a) gives the standard of comparison for the characteristics of flood under the conditions from b) to d).

Condition b) where the water-stage at a fixed position is held constant may be fulfilled practically in a reservoir exclusively used for electrification or at an estuary where the tidal stage variation is small.

Condition c) is fulfilled at the control section. In this paper we deal with the flood flow through a backwater reach which is bounded by a sharp-edged rigid weir, especially in the case where the backwater reach is on a small scale like the one created by sabo dam in an actual river.

Condition d) is fulfilled at a river junction or at a river mouth where the tidal stage variation is large. This case can be considered to be the application of cases b) and c). Although the combinations of the time lag of $h=h(t)$ at $x=l$ and $x=0$ or the shape of $h=h(t)$ are almost infinite, in this paper we discuss only a few typical cases.

2. Experimental equipment

(1) *The* 150 m *steel flume*

As shown in Fig. 1, the experimental equipment consisted of the flume, the supporting screw jacks, the reservoirs upstream and downstream, the returning pipe, the head tank, the gaging tank, the flood wave generator and the water stage controller downstream, etc.

The flume 60 cm wide, 60 cm deep and 150 m long, is made of steel and its bed is coated with cement mortar to eliminate the unevenness at the welding joints, and at the downstream end it has a pool 3 m wide, 3 m long and 1 m deep in which the water stage can be changed at will by controlling automatically the height of the 60 cm wide outlet overflow type weir. The flume is supported by the screwjacks at 6 m intervals and by adjusting these jacks the inclination of the flume can be changed from 0 to 1/150. A flood wave up to 100 l/s is generated by the pneumatic automatic control which opens and closes the air valve inserted between the head tank and the gaging tank.

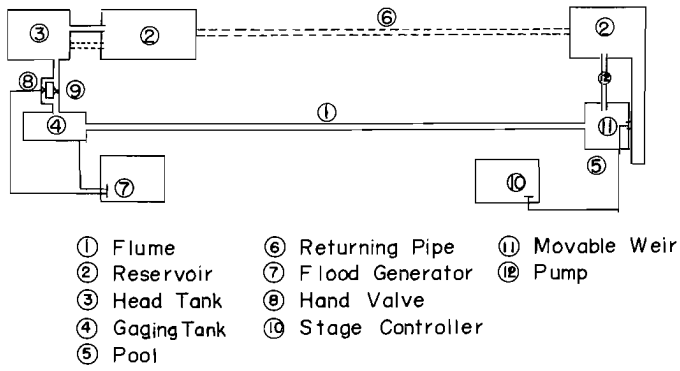

Fig. 1. The 150 m steel flume

This type of automatic control gives rise to discussion about the distortion between a programed flood and an actual one. With this equipment the discharge is distorted a little at the beginning of its rise, but as a whole the distortion is negligible and the ability of the discharge to reappear by the same program can be satisfied.

The accuracy of the water stage control at the downstream end is not very high especially when the flood wave is a very rapid one, because of the on-off operating mechanism of the stage controlling the outlet weir, but the equipment can be considered as having a satisfactory performance for examining the characteristics of the phenomena.

(2) *Measuring apparatuses*

The variation of the water stage was measured by a combination of the resistive wave meter and the dynamic strain meter and recorded by the electromagnetic oscillograph. This type of measuring apparatus gives rise to discussion about the linearity between the record and the actual variation and the change of sensitivity according to the variation of temperature. But examination reveals that the linearity is good, the change of sensitivity is about 2% per 1°C and the variation of temperature during an experiment is small, so the accuracy of the measuring of a stage is satisfactory.

The measurement of velocity was done by the pitot tube and the differential pressure gage of 20 gr/cm^2 at maximum and recorded by the electro-magnetic oscillograph through the dynamic strain meter.

3. Flood propagation through a uniform channel under the condition of $h \to 0$ at $x \to \infty$

Among many results of research concerning flood propagation through a uniform channel, the kinematic wave theory[1] and the diffusional theory,[3] which consider the mixing of great turbulence generated by the irregularity of a channel, are remarkable and by these theories the propagation speed and the quantity of attenuation of peak can be estimated. But they are confined to linear theory or

neglect the acceleration terms, and so on the effects of the nonlinearity or the acceleration terms much uncertainty remains.

In this section we examine the characteristics of the flood wave in a uniform channel and try to give the basis for a discussion on flood waves under various kinds of boundary condition.

(1) *Experimental procedure*

The kinds of experiment are shown in Table 1. The shapes of the $h-t$ curves on the steady base flow discharge are parabolic or triangular and these are very sharp compared with that which generally occurs in an actual river, but they have been adopted to facilitate an understanding of the effects of the acceleration terms.

TABLE 1. The kinds of experiment in the uniform channel

Run	Base Discharge (l/s)	Max. Discharge (l/s)	Duration Time	Arrangement of stations
1— 1	5	31.5	7′30″	1
1— 2	5	41.5	13′00″	1
1— 3	5	51.5	14′00″	1
1— 4	5	40.5	5′30″	1
1— 5	5	49.5	6′00″	1
1— 6	5	28.7	2′20″	2
1— 7	5	36.5	2′40″	2
1— 8	5	15.5	6′40″	2
1— 9	5	25.5	7′00″	2
1—10	5	31.0	6′40″	2
1—11	5	35.0	7′00″	2
1—12	5	40.0	7′30″	2
1—13	10	26.0	6′30″	2
1—14	10	30.7	7′30″	2
1—15	10	36.0	7′50″	2
1—16	10	40.0	7′10″	2

TABLE 2. The arrangement of measuring stations

	No. 1	No. 2	No. 3	No. 4	No. 5	No. 6	No. 7	No. 8	No. 9	No. 10
1	17m	32	56	73	98	119	133			
2	18m	34	50	60	65	70	88	98	118	137

The slope of the flume is 1/500, and the Manning roughness is $n=0.0116$ (m−sec).

The measurements of the water stage were taken at the stations shown in Table 2. The velocity was not measured.

(2) *Experimental results and considerations*

Fig. 2 shows an example of the variation of the stage-time relation curve. From this figure the characteristics of the deformation of the flood wave are not clear, but they become clear after the variation of the shape of the same phase has been examined against the distance.

We calculated the stage variation ratio ($\partial H/\partial t$) at the phase of which the stage height is $(1/2)h_{\max}$ and compared these values at each station in Figs. 3 and 4. These figures show that the wave become a little acuter or not so markedly deformed at the rising stage (corresponding to the positive value of $\partial H/\partial t$) except in the case of a very rapid wave (Run 1−6) and at the falling stage the wave becomes flatter against the distance.

From the linear theory we can not deduce this sharpening characteristic and so this may be a nonlinear effect. We will say more about the shape variation below.

In the wide rectangular uniform channel, if the Chézy type resistance law is adopted, the fundamental equation of flood flow is written as follows:

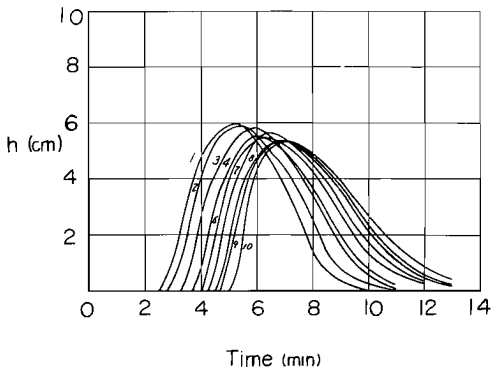

Fig. 2. Stage hydrograph (Run 1—1)

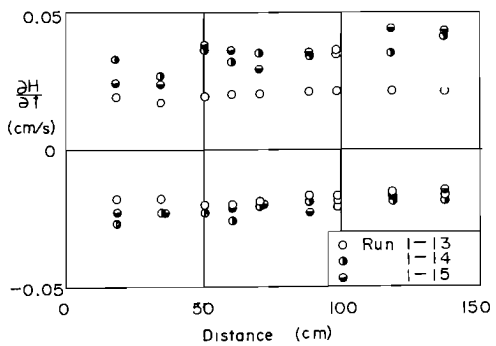

Fig. 4. Values of $\partial H/\partial t$ at the stage of $(1/2)h_{\max}$

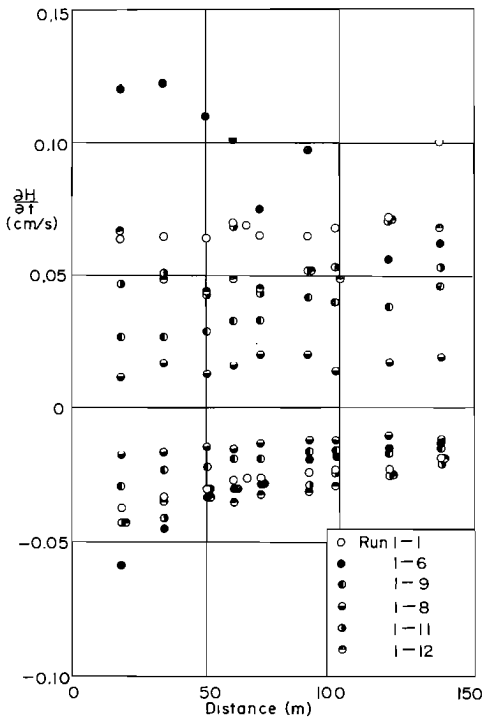

Fig. 3. Values of $\partial H/\partial t$ at the stage of $(1/2)h_{\max}$

$$\left\{1-\frac{F_r^2}{(1-\kappa)}\Phi\right\}\frac{\partial H}{\partial t}+V\left\{\frac{3}{2}-\frac{F_r^2}{(1-\kappa)}\left(3-\frac{\alpha_2}{2}-\frac{3}{2\alpha_1}\right)\Phi\right\}\frac{\partial H}{\partial x}$$
$$=\frac{q}{2(1-\kappa)i}\left\{1-(1-2\alpha_4+\alpha_3\alpha_4)F_r^2\right\}\frac{\partial^2 H}{\partial x^2} \quad \cdots\cdots(1)$$

where, F_r is the Froude number, H is the depth, V is the mean velocity, q is the discharge of unit width, i is the bed slope, $\alpha_1 V=-(\partial H/\partial t)/(\partial H/\partial x)$ (the propagation speed of the same depth), $\alpha_2 V=(\partial q/\partial t)/(\partial H/\partial t)$ (the propagation speed of the same discharge), $\alpha_3 V=(\partial^2 H/\partial t^2)/(\partial^2 q/\partial x^2)$ (the propagation speed of $\partial H/\partial t=const.$) $\alpha_4 V=(\partial^2 q/\partial x^2)/(\partial^2 H/\partial x^2)$ (the propagation speed of $\partial H/\partial x=const.$), $\Phi=(1/iV)(\partial H/\partial t)$ and $\kappa=\{\alpha_2-1/\alpha_1-(2-1/\alpha_1)F_r^2\}\Phi$.

At the beginning of the rising stage, the values of Φ or κ are large and the flow contains the characteristics of the long wave but this part diminishes rapidly and the main part of the flood propagates more slowly than the long wave and each phase propagates at approximately the same speed as the peak propagates.[3] For the first approximation, we assume the flood propagates as a kinematic wave, so that the propagation speed of the whole phase will be equal to $(3/2)V$, then $\alpha_1=\alpha_2=\alpha_3=\alpha_4=3/2$ and equation (1) will be

$$\left\{1-\frac{F_r^2}{(1-\kappa)}\Phi\right\}\frac{\partial H}{\partial t}+V\left\{\frac{3}{2}-\frac{F_r^2}{(1-\kappa)}\frac{5}{4}\Phi\right\}\frac{\partial H}{\partial x}$$
$$=\frac{q}{2(1-\kappa)}\left(1-\frac{1}{4}F_r^2\right)\frac{\partial^2 H}{\partial x^2} \quad \cdots\cdots(2)$$

From this equation we deduce the second approximation of the propagation speed ω of the same depth by neglecting the small terms,

$$\omega\fallingdotseq V\left[\frac{\frac{3}{2}-\frac{5}{4}\frac{F_r^2}{(1-\kappa)}\Phi}{1-\frac{F_r^2}{(1-\kappa)}\Phi}-\frac{\frac{2q}{q(1-\kappa)iV^3}\left(1-\frac{1}{4}F_r^2\right)\frac{\partial^2 H}{\partial t^2}}{\left\{1-\frac{F_r^2}{(1-\kappa)}\Phi\right\}\frac{\partial H}{\partial x}}\right] \quad \cdots\cdots(3)$$

At the main part of the flood wave, the values of Φ and κ are both sufficiently less than unity. So

$$\omega\fallingdotseq V\left[\frac{3}{2}+\frac{1}{4}\frac{F_r^2}{(1-\kappa)}\Phi+\frac{H}{3(1-\kappa)iV}\left\{1-\frac{1}{4}F_r^2+\frac{F_r^2}{(1-\kappa)}\Phi\right\}\frac{\frac{\partial^2 H}{\partial t^2}}{\frac{\partial H}{\partial t}}\right]$$
$$\fallingdotseq\frac{3}{2}CH^{\frac{1}{2}}i^{\frac{1}{2}}+\frac{1}{4}\frac{C^2}{g}\frac{\partial H}{\partial t}+H\left(\frac{1}{3i}-\frac{C^2}{12g}\right)\frac{\frac{\partial^2 H}{\partial t^2}}{\frac{\partial H}{\partial t}} \quad \cdots\cdots(4)$$

where C is Chézy's coefficient and g is the acceleration of gravity.

In equation (4), the first term of the right hand side acts to make the wave acute and if $\partial^2 H/\partial t^2<0$ when $\partial H/\partial t>0$, the third term acts to flatten the wave. And according to $\partial\omega/\partial H\gtrless 0$, the acumination and flattening of the wave are decided.

Now limiting the discussion to a fixed place and writing $\partial H/\partial t$ as $f(H)$, $\partial\omega/\partial H$ will be as follows:

$$\frac{d\omega}{dH}=\frac{3}{4}CH^{-\frac{1}{2}}i^{\frac{1}{2}}+\left(\frac{1}{3i}+\frac{C^2}{6g}\right)f'(H)+H\left(\frac{1}{3i}-\frac{C^2}{12g}\right)f''(H)\cdots\cdots\cdots(5)$$

where the prime means the derivative of H.

We can see by this equation that the acumination and flattening of the wave are decided by the relation between the functional form of $f(H)$ and the depth H.

Taking the Run 1−1 to be an example, we calculated equation 4 at station No. 1 as in Table 3. This result reveals that the celerity of each of the three stages is almost the same and the wave deforms little with propagation when there is in such a relation between $f(H)$ and H.

TABLE 3. Calculation of eq. (4) (Run 1—1, No. 1)

h	0.5cm	3cm	5cm
$\frac{\partial H}{\partial t}$	3.8×10^{-2}cm/sec	6.1×10^{-2}	3.0×10^{-2}
$\frac{\partial^2 H}{\partial t^2}$	1.61×10^{-3}cm/sec^2	-5.7×10^{-4}	-7.3×10^{-4}
$\frac{1}{4}\frac{C^2}{g}\frac{\partial H}{\partial t}$	0.022m/sec	0.044	0.024
$H\left(\frac{1}{3i}-\frac{C^2}{12g}\right)\frac{\frac{\partial^2 H}{\partial t^2}}{\frac{\partial H}{\partial t}}$	19.3×10^{-2}m/sec	-7.5×10^{-2}	-25.8×10^{-2}
$\frac{3}{2}CH^{\frac{1}{2}}i^{\frac{1}{2}}$	0.566m/sec	0.837	1.03
ω	0.781m/sec	0.806	0.800

As well as confirming the above-mentioned theoretical considerations, this result shows that the flood routing can be done by use of equation (4) if only the attenuation of the stage maximum is predicted by the other existing methods such as Hayashi s.[4]

The attenuation of the stage maximum of the experiments are shown in Fig. 5. In this figure the calculation results from Hayashi's method are also shown and

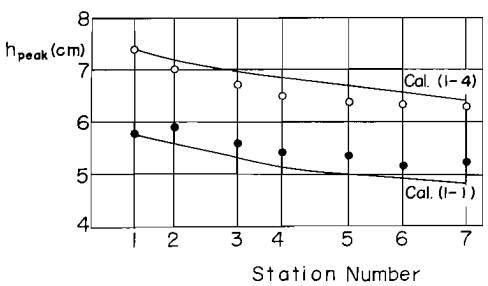

Fig. 5. Attenation of H_{peak}

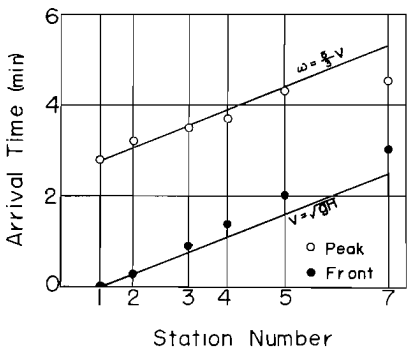

Fig. 6. Propagation of H_{peak} and front

considering the accuracy in deciding the value of $\partial^2 H/\partial t^2$ from the $h-t$ curve and the regularity of the channel, it can be said that the calculation has sufficient accuracy.

An example of the propagation speed of the stage maximum and front is shown in Fig. 6. In this figure the celerity of the $H_{\text{ピーク}}$ in the neighborhood of station No. 7 is very large because of the drawdown profile of the back water curve and except for this point the propagation of the $H_{\text{ピーク}}$ closely follows Kleitz-Seddon's law. The propagation speed of the front is less than that of a small disturbance and this result coincides with the well-known theoretical results.

Next, we try to compare the order of the terms in the equation of motion, where the discharge is calculated by the equation of continuity.

The equation of motion is

$$\frac{\partial H}{\partial x}=i\frac{1-\left(\frac{H_o}{H}\right)^2\left(\frac{R_o}{R}\right)^{\frac{4}{3}}+2\left(\frac{H_c}{H}\right)^3\frac{\frac{\partial H}{\partial t}}{Vi}-\frac{1}{gAi}\frac{\partial Q}{\partial t}}{1-\left(\frac{H_c}{H}\right)^3} \quad \cdots\cdots(6)$$

where suffix o, c shows the uniform and the critical flow respectively and R is the hydraulic radius, Q is the total discharge and A is the area of the section. The comparison of the order of the terms is shown in Table 4 for the Run 1—1, station No. 1. From this table we can conclude that for the first approximation of the equation of motion

$$\frac{\partial H}{\partial x}=i\frac{1-\left(\frac{H_o}{H}\right)^2\left(\frac{R_o}{R}\right)^{\frac{4}{3}}}{1-\left(\frac{H_c}{H}\right)^3} \quad \cdots\cdots(7)$$

TABLE 4. Comparison of order of terms in flood equation (Run 1—1)

	①	②	③	④	⑤	⑥	⑦	⑧
t	H(cm)	Q(l/s)	$\frac{\partial H}{\partial t}\frac{1}{Vi}$	$\left(\frac{H_0}{H}\right)^2\left(\frac{R_0}{R}\right)^{\frac{4}{3}}$	$\left(\frac{H_c}{H}\right)^3$	$2\left(\frac{H_c}{H}\right)^3\frac{\partial H}{\partial t}\frac{1}{Vi}$	$\frac{1}{gAi}\frac{\partial Q}{\partial t}$	$\frac{1}{i}\frac{\partial H}{\partial x}$
3′00″	3.05	7.0	0.359	1.18	0.516	0.370	0.410	−1.070
3′30″	4.60	13.5	0.578	1.12	0.520	0.600	0.468	−0.025
4′00″	6.40	21.0	0.486	1.00	0.410	0.298	0.359	−0.104
4′30″	7.60	27.5	0.232	1.025	0.492	0.299	0.226	−0.043
5′00″	8.20	31.0	0.198	1.097	0.500	0.198	0.093	−0.016
5′30″	8.70	31.5	−0.062	0.892	0.428	−0.053	−0.020	0.130
6′00″	8.40	30.5	−0.116	0.940	0.444	−0.103	−0.076	0.060
6′30″	7.90	27.8	−0.183	0.928	0.440	−0.161	−0.135	0.082
7′00″	7.20	23.5	−0.253	0.908	0.410	−0.207	−0.231	0.196
7′30″	6.40	18.5	−0.363	0.777	0.360	−0.262	−0.293	0.387
8′00″	4.90	12.2	−0.530	0.792	0.366	−0.388	−0.412	0.366
8′30″	4.00	7.0	−0.150	0.561	0.230	−0.228	−0.281	0.634
9′00″	3.20	5.5	−0.306	0.615	0.265	−0.161	−0.093	0.430

or

$$Q=\frac{1}{n}BHR^{\frac{1}{3}}\sqrt{i-\frac{\partial H}{\partial x}(1-F_r^2)} \quad \cdots\cdots(8)$$

is satisfactory, where n is Manning's roughness coefficient.

4. The flood propagation through a backwater reach which is bounded at the downstream end by a constant water depth under the condition of $h=0$ at $x=l$

In this section we try to study flood propagation under the most simple boundary condition where the water stage variation of the given place is zero. As mentioned in the introduction, this kind of boundary condition often occurs in an actual river and, furthermore, this section will become the basis of a study of flood flow under more complicated boundary conditions.

For these cases, the flood routing has been accomplished on the assumption that the inflow equals the outflow and that the maximum stage is calculated from a steady discharge corresponding to the maximum flood discharge. A study of the mechanism of the phenomena within a region, which is strongly affected by the boundary condition has not yet been undertaken.

(1) *Experimental procedure*

The kinds of experiment are shown in Table 5 and the slope of the flume is 1/500.

First the weir of the outlet was established at a suitable height when the base flow discharge of 5 l/sec was flowing and the water stage was maintained at constant while the experiment was being conducted. The measurment of the stage was taken at the stations shown in Table 6. The vertical velocity distribution was measured at the center of the sections.

TABLE 5. The kinds of experiment

Run	Base Discharge (l/s)	Max. Discharge (l/s)	Duration Time (min)	H_w (cm)
2—1—1	5	31.5	7	5.6
2—1—2	5	31.5	9	5.6
2—1—3	5	31.5	11	5.6
2—2—1	5	31.5	7	16.0
2—2—2	5	31.5	9	16.0
2—2—3	5	31.5	11	16.0
2—2—4	5	31.5	26	16.0
2—2—5	5	31.5	32	16.0
2—3—1	5	31.5	7	20.8
2—3—2	5	31.5	9	20.8
2—3—3	5	31.5	11	20.8

TABLE 6. The arrangement of measuring stations

	No. 1	No. 2	No. 3	No. 4	No. 5	No. 6	No. 7	No. 8	No. 9	No. 10
	18^m	34	56	78	88	98	110	120	135	147

(2) *Experimental results and considerations*

Fig. 7 shows an example of the stage variation at each station. When the boundary condition is completly fulfilled, the curve of station No. 10 must be the straight line $h=0$. Actually the stage changes, especially at the end of the flood, because of the mechanism of the operation of the stage controlling outlet weir, but up to the passage of the main part of the flood the variation is comparatively small, so we can consider the boundary condition as satisfied. An example of the water-level profile at every minute is shown in Fig. 8. In this figure the broken

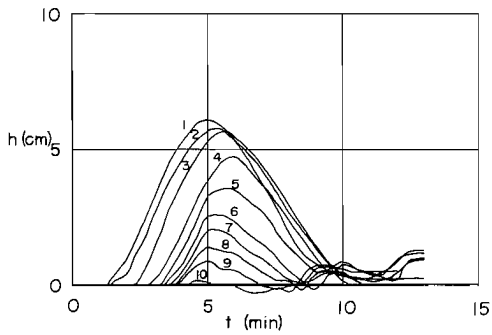

Fig. 7. Stage hydrograph (Run 2—3—2)

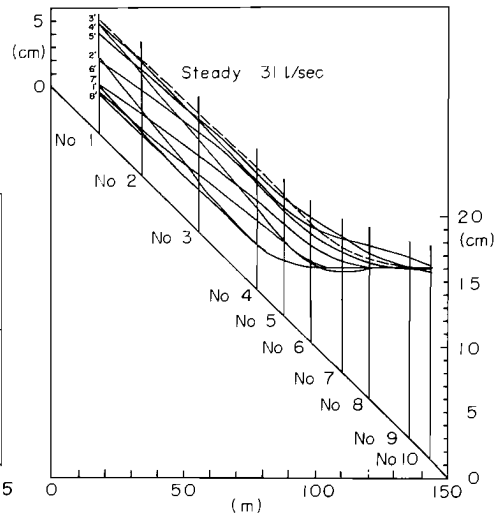

Fig. 8. Water-level profile (Run 2—2—1)

line shows the water-level corresponding to the steady discharge of 31 l/sec, which is the maximum flood discharge at the entrance to the region affected by the boundary condition. In the region upstream where the boundary codition is practically unaffected (uniform channel region), the acceleration terms are small comparing the water surface slope term and the friction term in the neighborhood of the peak, so that the maximum stage of the flood is near the steady stage. But in the backwater reach downstream the flood stage exceeded the steady stage. This phenomenon occurred with every experimental case and in Fig. 9 (1), (2) the maximum stage values measured from the stage of the base flow are shown. Hence, the idea hitherto held that the stage corresponding to the maximum steady discharge gives the safety side value is denied by the experiments. This may be

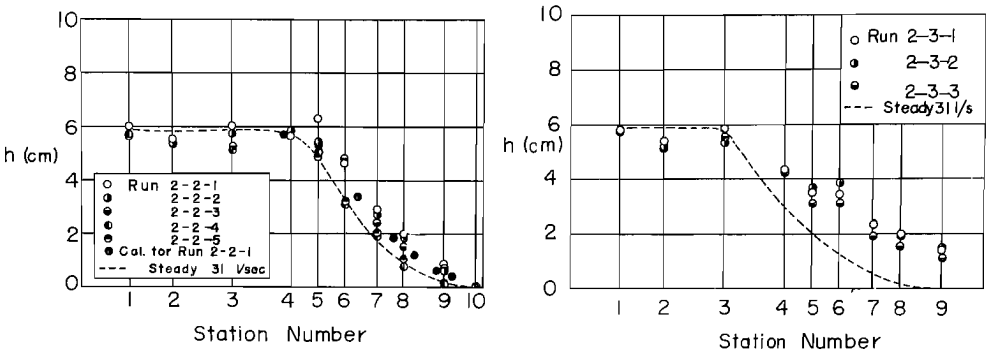

(1) (2)

Fig. 9. (1), (2) Diagram of H_{peak} attenuation in relation to distance

due to the effect of the accelaration term and we will say more about this point below.

Let's consider the stage variation in the neighborhood of the weir. Taking a notation like that in Fig. 10, the equations of motion and continuity in the wide rectangular section are

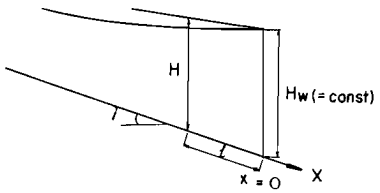

Fig. 10. Schematic diagram

$$\frac{\partial H}{\partial x}=\frac{i-\dfrac{q^2}{C^2H^3}-\dfrac{2q}{gH^2}\dfrac{\partial q}{\partial x}-\dfrac{1}{gH}\dfrac{\partial q}{\partial t}}{1-\dfrac{q^2}{gH^3}} \quad \cdots\cdots(9)$$

$$\frac{\partial H}{\partial t}+\frac{\partial q}{\partial x}=0 \quad \cdots\cdots(10)$$

Describing

$$H=H_1+H_2+\cdots\cdots, \qquad q=q_1+q_2+\cdots\cdots, \quad \cdots\cdots(11)$$

we can solve the equation by successive approximation.

The boundary conditions are for H_1 and q_1

$$\left.\begin{array}{ll} \text{at} & t=0, \quad H_1=H_0(x), \quad q_1=q_s \\ \text{at} & x=0, \quad H_1=H_w(=\text{const.}), \quad q_1=q_w(t) \end{array}\right\} \quad \cdots\cdots(12)$$

for H_2, H_3, ……, q_2, q_3,……

$$\left.\begin{array}{ll} \text{at} & t=0, \quad H_2=H_3=\cdots\cdots=0, \quad q_2=q_3=\cdots\cdots=0 \\ \text{at} & x=0, \quad H_2=H_3=\cdots\cdots=0, \quad q_2=q_3=\cdots\cdots=0 \end{array}\right\} \quad \cdots\cdots(13)$$

where q_s is the steady base flow discharge $H_0(x)$ is the depth corresponding to q_s.

In the neighborhood of the weir, the right-hand side of the equation (9) approximately equals i and for the first approximation,

$$\left.\begin{aligned} H_1 &= ix + H_w \\ q_1 &= q_w(t) \end{aligned}\right\} \quad \cdots\cdots(14)$$

can be adopted. Applying eq. (14) to the right-hand side of eq. (9), we can get H_2 which satisfies the given boundary and initial conditions (12), (13).

$$H_2 = \log\left[\left(\frac{ix+H_w+k}{H_w+k}\right)^{\left\{\frac{4\dot{q}_1}{6gi}-\frac{2}{k}\left(1-\frac{g}{C^2i}\right)\right\}}\left\{\frac{-\frac{q_1^2}{g}+H_w}{-\frac{q_1^2}{g}+(ix+H_w)}\right\}^{\left\{\frac{\dot{q}_1}{6gi}-\frac{k}{6}\left(1-\frac{g}{C^2i}\right)\right\}}\right]$$
$$+\frac{k}{\sqrt{3}}\left(1-\frac{g}{C^2i}\right)\tan^{-1}\frac{-2ix}{1+\frac{(2H_w-k)\{2ik+(2H_w-k)\}}{3k^2}} \quad \cdots\cdots(15)$$

where

$$k^3 = -\frac{q_1^2}{g} \quad \cdots\cdots(16)$$

In this region

$$ix \ll H_w, \quad (ix+H_w)^3 \ll H_w^3, \quad \frac{i}{H_w+k} \ll 1, \quad \frac{2i}{1+\frac{(2H_w-k)^2}{3k^2}} \ll 1$$

so eq. (15) can be transformed to

$$H_2 \approx \left\{\frac{2\dot{q}_1}{3gi}-\frac{k}{2}\left(1-\frac{g}{C^2i}\right)\right\}\frac{i}{H_w+k}x-\frac{k}{\sqrt{3}}\left(1-\frac{g}{C^2i}\right)\frac{6k^2i}{3k^2+(2H_w-k)^2}x \quad \cdots\cdots(17)$$

Hence, the stage variation in the neighborhood of the weir is as far as the second approximation,

$$H = H_w + Aix$$

where

$$A = \left[1+\left\{\frac{2\dot{q}_1}{3gi}-\frac{k}{2}\left(1-\frac{g}{C^2i}\right)\right\}\frac{1}{H_w+k}-\frac{k}{\sqrt{3}}\left(1-\frac{g}{C^2i}\right)\frac{6k^2}{3k^2+(2H_w-k)^2}\right] \quad \cdots\cdots(18)$$

Thus the stage variation in this region is approximately linear.

Now let's consider the moment which the maximum stage occurs at a given place. From the above discussion it is clear that when the maximum stage occurs the water surface slope at this place should be the maximum and so $\partial H/\partial x$ is the minimum. The value of $\partial H/\partial x$ when $\partial H/\partial t = 0$ is from eq. (9)

$$\frac{\partial H}{\partial x} = \frac{i-\frac{q^2}{C^2H^3}-\frac{1}{gH}\frac{\partial q}{\partial t}}{1-\frac{q^2}{gH^3}} \quad \cdots\cdots(19)$$

On the other hand, describing the depth corresponding to the steady flow H_s, when

$$\frac{\partial H_s}{\partial x} > \frac{\partial H}{\partial x} \quad \cdots\cdots(20)$$

the flood stage H exceeds the steady stage H_s, in which

$$\frac{\partial H_s}{\partial x}=\frac{i-\frac{q_s^2}{C^2H_s^3}}{1-\frac{q_s^2}{gH_s^3}} \quad \cdots\cdots(21)$$

For the case $q_s^2/qH_s^3=F_{rs}^2<1$, condition (20) will be satisfied when

$$\frac{q^2}{H^3}+\frac{1}{g}\frac{C^2(1-F_{rs}^2)}{1-\frac{C^2i}{g}}\frac{1}{H}\frac{\partial q}{\partial t}>\frac{q_s^2}{H_s^3} \quad \cdots\cdots(22)$$

That is, when the stage is maximum, if the value of $\partial q/\partial t$ is positive and sufficiently large, $H>H_s$ can be fulfilled. In these experiments this condition had to be satisfied. And at the position of the weir $H=H_s=H_w$ and $\partial H/\partial t=0$, so the condition (20) will be satisfied when

$$\frac{\partial q}{\partial t}>\frac{g\left(1-\frac{C^2i}{g}\right)}{C^2H_w^2(1-F_{rs}^2)}q_s^2\left(1-\frac{q^2}{q_s^2}\right) \quad \cdots\cdots(23)$$

The equation (23) contains H_w in the denominator, so when H_w is great, the flood stage can exceed the steady stage for a small value of $\partial q/\partial t$ and for the same discharge hydrograph, when the stage of peak is heigher the H_w is larger. These facts are shown in Fig. 9 (1), (2). If the isosceles triangular hydrograph with a base flow of 5 l/sec and a maximum discharge of 30 l/sec under $H_w=15$ cm is taken as an example, the condition (23) will be satisfied when the duration time is less than 32 minutes. This case corresponds to the Run 2−2−5 in Fig. 9 (1) and the experimental values are near the stage of the steady flow.

As is clear from the above consideration, the flood stage can exceed that of the steady only when the peak of the stage occurs earlier than the peak of the discharge. This phenomenon does not occur in the uniform channel.

Fig. 11 shows an example of the stage-discharge relationship and the direction of cirulation of the loop of the upper uniform channel region and of the downstream region is contrariwise. It is now necessary to show whether the direction of circulation of the loop is generally opposite to that of the uniform channel

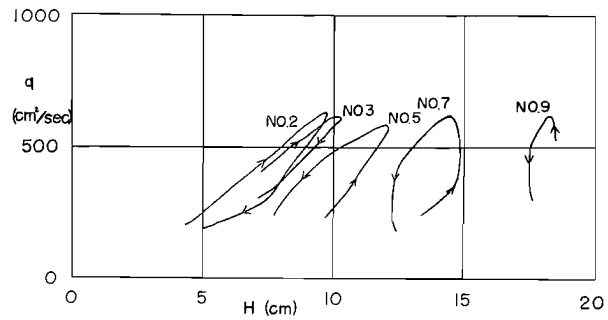

Fig. 11. Stage-discharge relationship

region in this case.

As $\partial/\partial t(\partial H/\partial X)=0$ at the moment when the stage is maximum, the following equation will be derived:

$$\frac{2q}{C^2H^3}\left(\frac{C^2i}{g}-1\right)\frac{\partial q}{\partial t}+\left(1-\frac{q^2}{gH^3}\right)\frac{2q}{gH^2}\frac{\partial^2 H}{\partial t^2}-\frac{1}{gH}\left(1-\frac{q^2}{gH^3}\right)\frac{\partial^2 q}{\partial t^2}$$
$$-\frac{2q}{g^2H^4}\left(\frac{\partial q}{\partial t}\right)^2=0 \quad \cdots\cdots(24)$$

(24) is the quadratic equation of $\partial q/\partial t$ and if this equation has two opposite sign solutions, $\partial q/\partial t$ is larger than zero when the stage maximum occurs and the direction of circulation is opposite to that in the uniform channel. In the case of $F_r^2=q^2/gH^3<1$, the above condition will be satisfied when

$$\frac{\partial^2 H}{\partial t^2}\left(1-\frac{H}{2q}\frac{\frac{\partial^2 q}{\partial t^2}}{\frac{\partial^2 H}{\partial t^2}}\right)>0 \quad \cdots\cdots(25)$$

In the above inequality $(\partial^2 q/\partial t^2)/(\partial^2 H/\partial t^2)$ is the propagation velocity of the same value of $\partial q/\partial t$ and if this is greater than twice the particle velocity q/H, (25) will be satisfied because $\partial^2 H/\partial t^2<0$ when the H_{peak} occurs. In a backwater region bounded by a constant water depth, the stage variation is small and so the quantity of storage is small, especially when the area of the reservoir is small. Consequently the pattern of the discharge hydrograph does not become greatly distorted and the propagation velocity of the discharge is very rapid; then $(\partial^2 q/\partial t^2)/(\partial^2 H/\partial t^2)$ is greater than $2q/H$ and the inequality (25) will be always satisfied in this region.

Fig. 12 (1), (2), (3) explains the propagation of the front and peak of the stage and discharge. The propagation of the front has the characteristics of the same

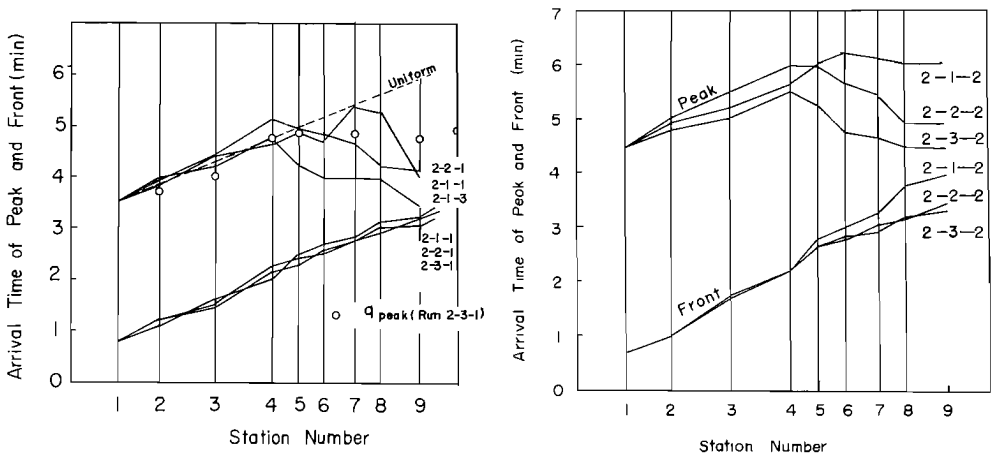

(1) (2)

Fig. 12. (1), (2) Propagation of peak and front

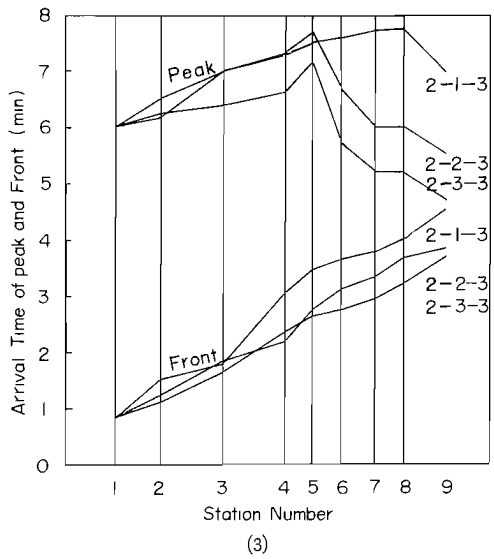

(3)

Fig. 12. (3) Propagation of peak and front

kinds mentioned in section 3. The acceleration term plays an important role in the propagation speed of the front and when the speed is higher the rising stage rate of the front is steeper. In the uniform channel region the propagation of the peak follows Kleitz-Seddon's law, but in the backwater reach the peak occurs downstream previous to upstream. Within the limits of these experiments, the values of $\partial q/\partial t$ at the stage maximum are from eq. (24)

$$\left.\begin{aligned}\frac{\partial q}{\partial t}=H\Bigg\{&\frac{g^2}{2C^2}\left(\frac{C^2i}{g}-1\right)\\&+\sqrt{\left\{\frac{g^2}{2C^2}\left(\frac{C^2i}{g}-1\right)\right\}^2+g\left(1-\frac{q^2}{gH^3}\right)\frac{\partial^2 q}{\partial t^2}\left(\frac{1}{\omega}-\frac{H}{2q}\right)}\Bigg\}\end{aligned}\right\}\quad\cdots\cdots\cdots\cdots(26)$$

in which

$$\omega=\frac{\dfrac{\partial^2 q}{\partial t^2}}{\dfrac{\partial^2 H}{\partial t^2}}$$

and because the depth is larger downstream, the stage maximum occurs earlier downstream than upstream.

The reduction of the discharge maximum following the propagation is

$$\frac{dq}{dx}=\frac{\partial q}{\partial x}=-\frac{\partial H}{\partial t}\quad\cdots\cdots\cdots\cdots\cdots\cdots\cdots\cdots\cdots\cdots\cdots\cdots\cdots\cdots\cdots\cdots\cdots\cdots(27)$$

because $\partial q/\partial t=0$ at the discharge maximum and when $\partial q/\partial t=0$, it is clear from the above discussion that $\partial H/\partial t<0$, so that the discharge increases against distance travelled under this type of boundary conditions. This phenomenon can be exp-

lained more clearly as follows. The peak of the stage occurs earlier than the discharge maximum, therefore the maximum of the storage occurs before the maximum discharge flows in and the propagation of discharge is delayed at this state of rising discharge, but later the stored quantity together with the larger flow-in dischage flows out, so that the discharge maximum increases. Then if the storage area is small, the discharge increasing effect is small and within the limits of these experiments the discharge is always smaller than that of the generated flood hydrograph at the upstream end.

From eq. (26) we can get the approximate value of the maximum depth at a given position in the backwater reach. That is, comparing $1/\omega$ with $H/2q$ we neglect the former and consider that the discharge hydrograph does not change its shape in this region, then we can find the depth which satisfies the equation (26) by the graphical solution and the distance l from the downstream end of this stage is

$$l=\frac{(H_w-H)\left\{1-\left(\frac{H_c}{H}\right)^3\right\}}{i\left\{1-\left(\frac{H_o}{H}\right)^3-\frac{1}{gHi}\frac{\partial q}{\partial t}\right\}} \quad \cdots\cdots(28)$$

The full circle in Fig. 9 (1) is the calculated value for the Run 2−2−1. The calculated results do not correspond well to the experiment but they explain approximately the tendency of the phenomena.

5. Flood propagation through a backwater reach bounded by a rigid weir under the condition of $h=h(q)$ at $x=l$

Flood propagtion through this type of boundary condition has been dealt with in relation to that through a large scale reservoir.[5,6] But when the reservoir is small, the water surface slope greatly diverges from the horizontal during the flood and what is called the transition reach takes the greater part of the backwater reach. The propagation characteristics through a transition reach are still obscure and we will study the characteristics in such a case.

(1) *Experimental procedure*

The disposition of the measuring stations and the kinds of experiment are shown in Tables 7 and 8 respectively. At the station 143 m we set two kinds of sharp edged rectangular weir of which the width of overflow is 60 cm and 30 cm and the heights are 10 cm or 15 cm. The slope of the flume is 1/500.

TABLE 7. The arrangement of measuring stations

	No. 1	No. 2	No. 3	No. 4	No. 5	No. 6	No. 7	No. 8	No. 9	No. 10
for Run 3-2-, 3-3-	17m	32	56	73	98	119	143			
for Run 3-4-1	17m	34	56	68	78	88	98	110	120	143

TABLE 8. The kinds of experiment

Run	Base Discharge (l/s)	Max. Discharge (l/s)	Duration Time (min)	weir
3—2—1	5	30	5	Height 10cm
3—2—2	5	40	5	Breadth 60cm
3—2—3	5	50	10	
3—3—1	5	30	5	Height 15cm
3—3—2	5	40	5	Breadth 60cm
3—3—3	5	50	10	
3—4—1	5	30	5	Height 10cm Breadth 30cm

(2) *Experimental results and considerations*

An example of the stage hydrograph is shown in Fig. 13. From this figure we can see that, in the region some distance upstream of the weir, the stage varies approximately with the same phase after the stage maximum occurs. This region is the so-called storage region where the water level is nearly horizontal. The curve of station No. 4 has two peaks corresponding to the condition upstream and downstream, i. e., at station No. 4 the flood has the characteristics of a uniform channel flood in the rising stage and in the falling stage it has the characteristics of the storage region. Thus station No. 4 is in the transition region. The characteristics of the celerity of the stage maximum differ in respect to the upstream and downstream section of this station. To explain this fact more clearly we show the arrival time of the stage maximum at each station in Fig. 14. In the cases where the overflow width is the same as the channel width the places where the propagation characteristics change differ according to the weir height but at the position of the weir the stage max. occurs approximately at the same time. The arrival time is also approximately the same as that calculated by Kleitz-Seddon's law which corresponds to the celerity in the uniform channel.

In the case where the overflow width is half the channel width the arrival time of the stage max. is delayed compared with the uniform channel. The

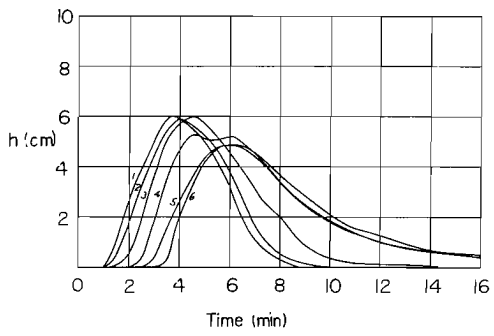

Fig. 13. Stage hydrograph (Run 3—2—1)

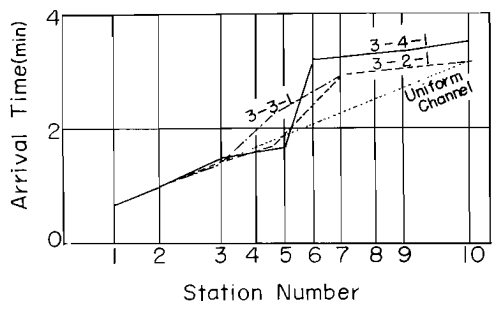

Fig. 14. Popagation of H_{peak}

celerity of the stage max. in the storage region is very large and in these cases is larger than the celerity of the long wave. In Fig. 15 the propagation of the discharge max. is shown. In this figure the full line shows Kleitz-Seddon's law in the uniform channel and the broken line shows that in the storage region in which the discharge is calculated by the storage equation. From this figure we can see that in the cases where the overflow width is the same as the channel width, the propagation of discharge is approximately the same as that of the uniform channel and in the storage region Kleitz-Seddon's law is also applicable. The reason for these propagation characteristics is as follows:

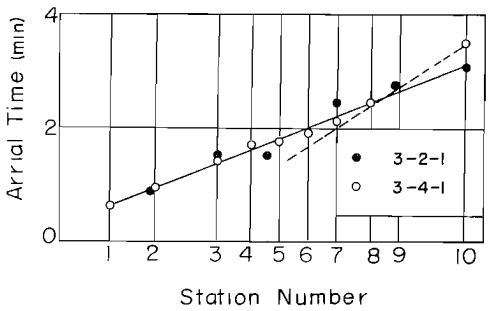

Fig. 15. propagation of the q_{max}.

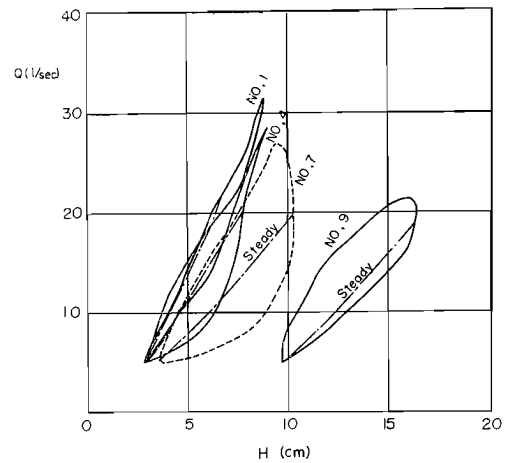

Fig. 16. Stage-discharge relationship (Run 3—4—1)

As is clear from Fig. 16, the $H-Q$ relation in the transition reach is close to that of the uniform channel in the rising stage and in the falling stage it is close to that of the storage reach. In the uniform channel the $H-Q$ relation is close to that of the steady flow and in the cases where the overflow width is the same as the channel width, the tangent of the $H-Q$ relation dQ/dA of the steady flow is approximately the same as that of the uniform channel. In the case of the 60 cm wide weir, the storage reach is short and so the propagation characteristics of the stage maximum and discharge maximum are approximately the same. On the other hand in the case of the 30 cm wide weir the value of dQ/dA of the steady flow is different from that of the uniform channel, so the arrival time of the peak is different from that of the uniform channel.

To make clear the sedimentation problem of the reservoir, we need to know the distribution of the tractive force during the flood, especially the movement of the point of the abrupt change of the water surface slope, i. e., the movement of the boundary of the storage reach and the transition reach.

The one dimensional equation of motion of the unsteady flow is eq. (6) and the order of the terms in eq. (6) for the case of Run 3−2−1 is shown in Table 9 in which ε is the value defined as

TABLE 9. Comparison of order of terms in flood equation

①	②	③	④	⑤	⑥	⑦	⑧	⑨	⑩
No.	t	H(cm)	Q(l/s)	$\frac{\partial H}{\partial t}\frac{1}{Vi}$	$\left(\frac{H_0}{H}\right)^2\left(\frac{R_0}{R}\right)^{\frac{4}{3}}$	$\left(\frac{H_c}{H}\right)^3$	$2\left(\frac{H_c}{H}\right)^3\frac{\partial H}{\partial t}\frac{1}{Vi}$	$\frac{1}{gAi}\frac{\partial Q}{\partial t}$	ε
3	5′00″	2.5	5.0	0	1.09	0.439	0	0	0.84
	6′00″	3.5	9.5	0.25	1.19	0.632	0.35	0.307	1.40
	8′00″	7.8	30.0	0.192	1.16	0.539	0.162	0.100	1.21
	8′30″	8.1	31.0	0	1.12	0.580	0	−0.0577	1.15
	9′00″	7.5	27.0	−0.167	1.06	0.486	−0.135	−0.179	1.03
	10′00″	6.5	19.5	−0.267	0.833	0.386	−0.212	−0.153	0.824
	11′00″	4.9	11.5	−0.233	0.754	0.320	−0.191	−0.158	0.686
	12′00″	3.6	7.5	−0.150	0.815	0.355	−0.153	−0.118	0.767
	13′00″	2.8	5.0	−0.10	0.779	0.313	−0.105	−0.101	0.684
5	6′00″	3.2	5.0	0	0.522	0.210	0	0	0.395
	6′30″	3.3	5.5	0.36	0.584	0.239	0.172	0.14	0.615
	8′00″	6.4	20.0	0.240	0.927	0.422	0.202	0.336	1.105
	9′00″	7.7	27.0	0.128	0.970	0.449	0.115	0.0736	0.871
	10′00″	8.2	26.0	0	0.751	0.344	0	−0.0692	0.515
	11′00″	7.4	21.5	−0.198	0.672	0.317	−0.126	−0.0958	0.564
	12′00″	6.2	16.5	−0.197	0.681	0.323	−0.127	−0.103	0.564
	14′00″	4.4	9.0	−0.158	0.605	0.286	−0.0904	−0.0800	0.460
	16′00″	3.6	5.5	−0.646	0.449	0.185	−0.239	−0.0277	0.320
6	6′30″	7.4	5.0	0	0.0425	0.0170	0	0	0.025
	7′00″	7.6	5.5	0.448	0.0482	0.0197	0.07	0.07	0.083
	8′00″	10.0	17.5	0.800	0.185	0.0852	0.136	0.163	0.139
	9′00″	12.2	25.0	0.268	0.205	0.0967	0.0518	0.0639	0.132
	9′30″	12.5	27.0	0.0926	0.227	0.105	0.0195	0.0136	0.130
	10′00″	12.5	26.5	−0.0590	0.216	0.101	−0.0119	−0.0397	0.095
	10′30″	12.25	25.0	−0.184	0.203	0.0954	−0.0351	−0.0405	0.113
	11′00″	11.9	22.5	−0.238	0.170	0.0835	−0.0397	−0.0595	0.075
	12′00″	10.8	17.5	−0.341	0.157	0.0674	−0.0460	−0.0617	0.080
	13′00″	9.7	13.0	−0.412	0.121	0.0523	−0.0431	−0.0584	0.057
7	7′00″	12.4	5.0	0	0.0090	0.00358	0	0	0.005
	7′30″	13.1	7.5	2.19	0.0168	0.00753	0.0329	0.054	0.03
	8′00″	14.5	13.5	1.61	0.0359	0.0195	0.0627	0.107	0.062
	8′30″	15.9	19.0	0.837	0.0563	0.0249	0.0415	0.0892	0.080
	9′00″	16.8	24.0	0.456	0.0720	0.0340	0.0310	0.0506	0.060
	9′30″	17.2	26.0	0.165	0.0790	0.0373	0.0123	0.0247	0.057
	10′00″	17.4	27.0	−0.064	0.0840	0.0390	−0.00501	0	0.050
	10′30″	17.1	26.0	−0.230	0.0806	0.0379	−0.0174	−0.0249	0.036
	11′00″	16.7	23.5	−0.391	0.0725	0.0328	−0.0256	−0.0595	0.007
	12′00″	15.5	18.5	−0.461	0.0561	0.0257	−0.0237	−0.0366	0.017
	13′00″	14.6	13.5	−0.432	0.0356	0.0164	−0.0142	−0.0388	0
	14′00″	13.8	10.0	−0.517	0.0307	0.0111	−0.0115	−0.0291	0.001
	15′00″	13.1	7.5	−0.524	0.0170	0.00741	−0.00777	−0.0216	0
	16′00″	12.7	6.0	−0.208	0.0125	0.00518	−0.00215	−0.0112	0
	17′00″	12.6	5.0	−0.126	0.0086	0.00344	−0.000867	0	0
	18′00″	12.5	5.0	−0.062	0.0087	0.00351	−0.000439	0	0

$$\varepsilon=1-\frac{\frac{\partial H}{\partial x}}{i} \quad \cdots\cdots(29)$$

In the transition reach each term is of the same order and in the storage reach each term is also of the same order but each is sufficiently smaller than unity and so approximately

$$\frac{\partial H}{\partial x}=i \quad \cdots\cdots(30)$$

If we define $\varepsilon \leqq 0.1$ as the index of the storage reach, the boundary of the storage reach is between Nos. 5 and 6 for the case of Run 3−2−1. Strictly speaking, to get value of ε, each term of eq. (6) must be considered because each is of the same order, but the value of ε changes abruptly with the change of the value of column 6 and in practice, neglecting the acceleration terms, ε may be calculated by

$$\varepsilon=\frac{\left(\frac{H_o}{H}\right)^2\left(\frac{R_o}{R}\right)^{\frac{4}{3}}-\left(\frac{H_c}{H}\right)^3}{1-\left(\frac{H_c}{H}\right)^3} \quad \cdots\cdots(31)$$

and when the section is wide and rectangular,

$$\varepsilon=\frac{\left(\frac{H_o}{H}\right)^3-\left(\frac{H_c}{H}\right)^3}{1-\left(\frac{H_c}{H}\right)^3} \quad \cdots\cdots(32)$$

The length l of the storage reach is then decided, referring to Fig. 17, by replacing ε as unity in the following equation:

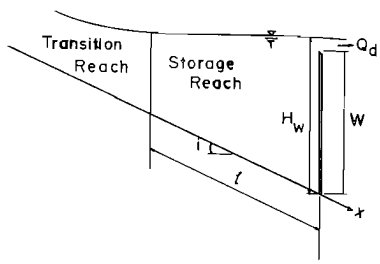

Fig. 17. Schematic diagram

$$\frac{\left(Q_d+B\frac{\partial H}{\partial t}l\right)^2}{C^3B^2i(H_w-il)}=\frac{0.1}{1-0.9\left(\frac{C^2i}{g}\right)} \quad \cdots\cdots(33)$$

From this equation we can calculate the value of l and compare the calculated l and the observed l in Fig. 18. The inner part and upstream part of this loop where it is affected by the boundary condition can be defined as the transition

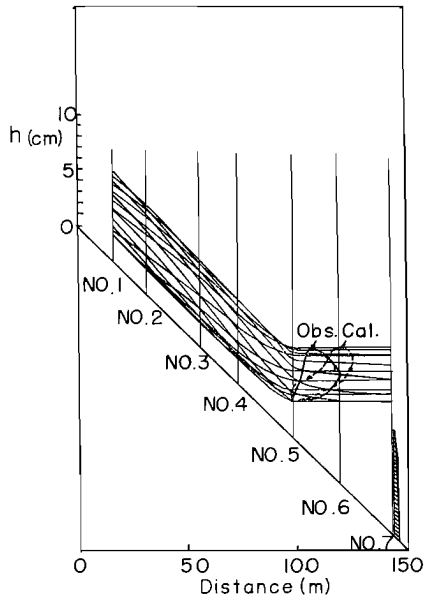

Fig. 18. Water-level profile (Run 3—2—1)

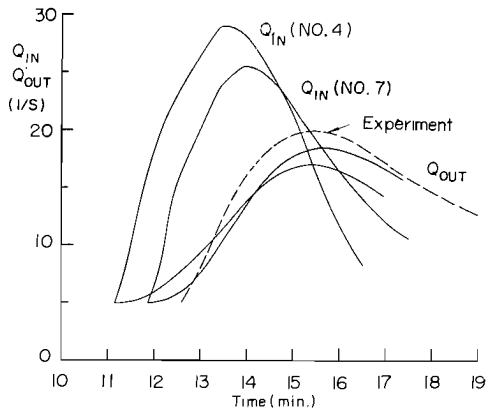

Fig. 19. Comparison between graphical solution of Q_{out} and experiment (Run 3—4—1)

reach.

Next, we will discuss whether the hitherto graphical calculating method of the out-flow discharge, which assumes the water-level to be horizontal, is still valid in the case of a small scale backwater reach. Prior to the calculation, we need to decide the position of entrance of the reservoir and the discharge hydrograph at that position but quantitative effect of the transition reach is still obscure. And so we assume that the entrance is the upstream end of the storage reach at the front of the flood and the storage effect is the same as the uniform channel reach. Fig. 19 shows the comparison between the graphical solution and the experiment for the case of Run 3−4−1. Station No. 4 can be considered to be the entrance of the transition reach and the hydrographs Q_{in} (No. 4) and Q_{in} (No. 7) are the values calculated by the equation of continuity. This figure shows that if the weir is low and the transition reach is comparatively large the hitherto graphical solution is inapplicable.

6. Flood propagation through a river junction or an estuary under the condition of $h=h(t)$ at $x=l$

It is very difficult to solve generally the flood phenomena in these cases, but for a few particular cases, there are some examples of analytical and experimental studies, especially for the cases of the running up of the tide or storm surge into a steady flowing river. But previous studies assume the special resistance law or the uniformity of the peculiar river flow. So we need to grasp the characteristics of the flow experimentally.

(1) *Experimental procedure*

The kinds of experiment are shown in Table 10. First we examine the cases where the peculiar river discharge is steady and then we examine the cases of flood flow where the stage variation of the downstream is the same as in the first group of experiments. The disposition of the measuring station is shown in Table 6 and the slope of the flume is 1/500.

TABLE 10. The kinds of experiment

Run	Flood Wave			Downstream Stage			Time Lag of Peaks Upstream and Downstream (min)
	Base Discharg (l/s)	Max. Discharge (l/s)	Duration Time (min)	Initial Depth (cm)	Max. Depth (cm)	Duratim Time (min)	
4—1—1	5	5		11	17.4	14	
4—2—1	5	5		11	23.0	14	
4—1—2	9.5	9.5		11	17.4	14	
4—2—2	9.5	9.5	Steady	11	23.0	14	
4—1—3	20.5	20.5	Flow	11	17.4	14	
4—2—3	20.5	20.5		11	23.0	14	
4—1—4	30.5	30.5		11	17.4	14	
4—2—4	30.5	30.5		11	23.0	14	
4—1—5	5	31.5	7	11	17.4	14	1
4—2—5	5	31.5	7	11	23.0	14	1
4—1—6	5	31.5	9	11	17.4	14	1
4—2—6	5	31.5	9	11	23.0	14	1
4—1—7	5	31.5	7	11	17.4	14	5
4—2—7	5	31.5	7	11	23.0	14	5
4—1—8	5	31.5	9	11	17.4	14	5
4—2—8	5	31.5	9	11	23.0	14	5

(2) *Experimental results and considerations*

Fig. 20 shows the celerity of running up of the front in the case of a steady river discharge. The celerity is less than that of the disturbance ($\sqrt{gH}-V$) for each case, but the shallower the depth of the flow (the smaller the value V), the greater the celerity. For the same depth, the greater the stage rising rate (the larger the acceleration terms), the larger the celerity of running up. Fig. 21 shows the celerity of peaks. The celerity of the peak is larger than that of the front but the propagation characteristics have the same tendency. Following the results of Yano and others,[7] if the peculiar discharge is constant and the flow is uniform the wave heights attenuate exponentially upstream but when the waves run up the backwater reach, the wave heights do not attenuate exponentially as shown in Fig. 22. From this figure we can also see that the larger the discharge, the larger the rate of subsidence and, for the same discharge, the smaller the wave height (the smaller the acceleration terms), the smaller the rate of subsi-

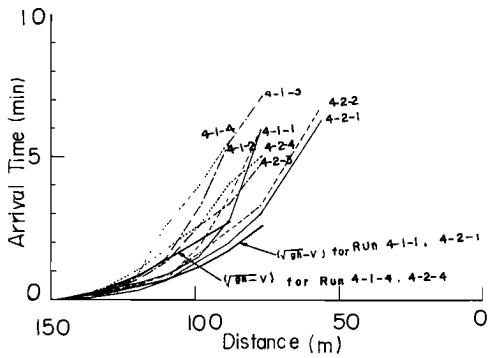

Fig. 20. The running up celerity of the front

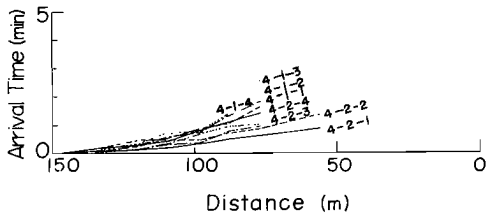

Fig. 21. The running up celerity of the peak

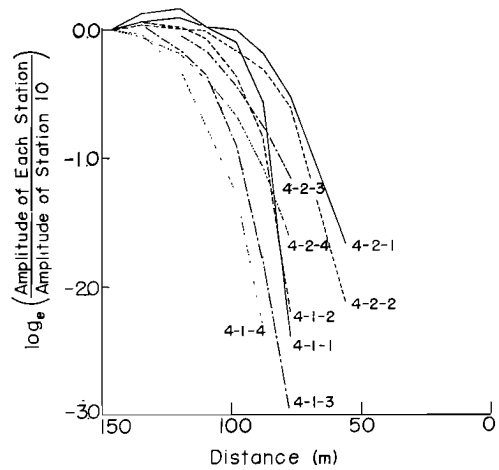

Fig. 22. Attenuation of H_{peak}

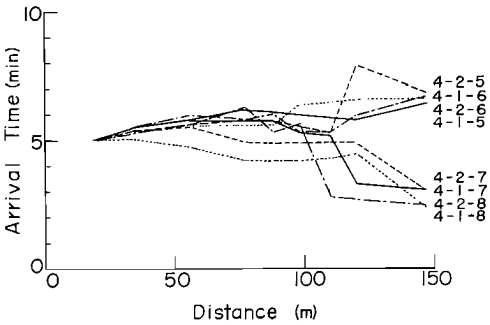

Fig. 23. Propagation of peak

dence. It is noteworthy that when the discharge is not very great, the wave height increases near the downstream end.

Fig. 23 shows the propagation of the h_{peak} for the case where the peculiar discharge is unsteady. The time of the occurrence of the peak at stations Nos. 1 and 10 is given at will. One group of experimeriments deals with the cases where the peak upstream occurs before that downstream and another group deals with the cases where the peak downstream occurs first. The propagation of the flood is greatly affected by the downtsream stage variation and little affected by the flood hydrograph within the limits of these experiments.

When the stage variation downstream is independent of the flow-in hydrograph as in these experiments, there are cases where the outflow discharge is greater than the flow-in discharge because of the addition of the storage by the downstream stage variation. It is expected on these occasions in reference to the considerations set out in section 4 that the stage maximum of a flood can be higher

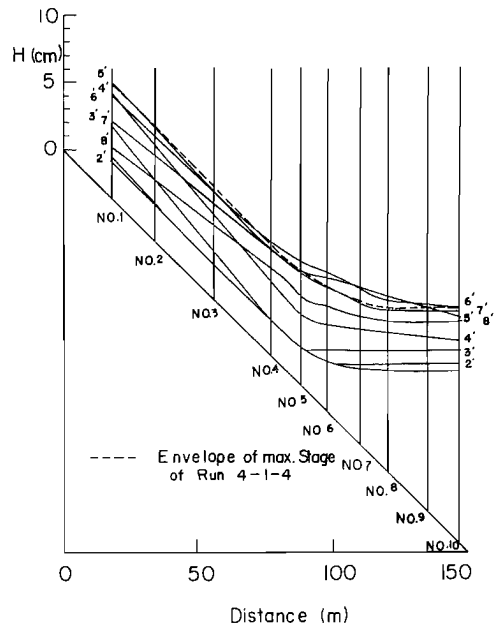

Fig. 24. Water-level profile (Run 4—1—4)

than that of a steady flow. Fig. 24 reveals this fact. In this figure the broken line shows the envelope of the stage maximum of the Run 4−1−4.

Under this condition the theoretical analysis of the flood is very difficult and for an actual river the quantitative analysis can be performed for the time being only by computor calculation. But to establish the fundamental equations to be calculated, it is necessary to perform more accurate experiments.

7. Conclusion

The authors have studied experimentally and theoretically the characteristics of flood flow under various boundary conditions from the viewpoint of the effects of the accleration terms in the equation of motion.

Thus, in section 3, as well as confirming the theoretical results arrived at hitherto, they have made clear that the flood wave receives simultaneously the flattening effect of the diffusion and the sharpening effect of the nonlinearity and according to the pattern of the hydrograph, the wave may become acute with propagation at the rising stage.

In section 4, they have dealt with the flood flow through a backwater reach which is bounded by a constant water depth and they have discovered many characteristics which are different from the uniform channel flood. For example, if the rate of increase of the discharge is rapid enough, the stage is higher than that of the steady flow corresponding to the maximum discharge of the flood. The peak of the stage occurs before the occurrence of the discharge maximum.

The propagation speed of the stage max. and of the discharge is very high and under some conditions the stage max. occurs downstream before it appears upstream. The deformation of the hydrograph is small. The authors have succeeded in explaining these characteristics and have found the condition under which the stage of the flood exceeds the steady stage.

In section 5, the authors have studied flood flow bounded by a rectangular sharp-edged weir. They have confirmed that the backwater reach can be divided into two regions, one being the storage region and the other the transition region. They have discussed the propagation characteristics in these regions and from these discussion they have made clear that for the time lag of peak propagation, the overflow condition plays an important role and if the gradient of the tangent of the stage-discharge relation curve in the uniform channel region is approximately the same as that at the weir, the arrival time of the peak at the station of the weir is about the same whether the weir is there or not. Moreover they have derived the equation for calculating the length of the storage region practically and they have made clear that if the storage region is small as was the case in these experiments, the previous graphical solution of the storage equation is inaccurate because for that case the transition region has a great effect, but the quantitative properties in the transition reach are still obscure.

In section 6, the authors have dealt with the cases where the flood propagates through a boundary condition corresponding to a river junction or estuary. First they have examined the running up of the downstream boundary condition into a steady river flow and secondly they have examined a unsteady river flow. To discuss the characteristics in these cases is generally very difficult and many problems are left for future study.

Acknowledgements

The authors are greatly indebted to Professor Katsumasa Yano of Kyoto University, for his constant instruction during this study and thanks are also due to Mr. Tadashi Takemoto for his assistance in the experiments and computations.

References

1) Lighthill M. J. and Whitham G. B.: On Kinematic Waves, I, Flood movement in long rivers, Proc. Roy. Soc. of London, vol. 229, 1955, pp. 281-316.
2) Hayami S.. On the propagation of flood waves, Disaster Prevention Research Institute, Kyoto Univ. Bulletin No. 1, 1951.
3) Stoker J. J.. Water Waves, Interscience, 1965, pp. 505-509.
4) Hayashi T.: Mathematical Theory and Experiment of Flood Waves, Trans. Japan Soc. of Civil Eng. No. 18, Sept. 1953, pp. 13-26.
5) Ishihara Y. and Kishida T.. On the flood control by reservoir and its synthetic effects on the flood flow for the river reach below the reservoir, Disaster Prevention Research Institute Bulletin Memorial issue of the fifth anniversary Nov. 1956, pp. 201-210 (in Japanese)
6) Yano K. and Adachi S.: Experimental study on the propagation of flood wave through reservoir, Disaster Prevention Research Institute Bulletin Memorial issue of the fifth anniversary Nov. 1965, pp. 211-219 (in Japanese)
7) Yano K., Adach S., Okuda S., Higuch H. and Daido A.: Model experiment of Neya river Fundamental method for operating the Konoike weir, Disaster Prevention Research Institute Bulletin Memorial issue of the fifth anniversary Nov. 1956, pp. 241-272 (in Japanese)